



The Effect of Vehicle Body Shapes on the Near Wake Region and Drag Coefficient: A Numerical Study

Hayder Kareem Sakran

Assistant Lecturer

College of Engineering- University of AL Muthanna

E-mail:hsakran@my.bridgeport.edu

ABSTRACT

The purpose of this paper is to gain a good understanding about wake region behind the car body due to the aerodynamic effect when the air flows over the road vehicle during its movement. The main goal of this study is to discuss the effect of the geometry on the wake region and the aerodynamic drag coefficient. Results will be achieved by using two different shapes, which are the fastback and the notchback. The study will be implemented by the Computational Fluid Dynamic (CFD) by using STAR-CCM+[®] software for the simulation. This study investigates the steady turbulent flow using k-epsilon turbulence model. The results obtained from the simulation show that the region of the air separation behind the vehicle varies with the variation of the body design. The minimum drag coefficient can be achieved with notch-back since the separation of the air is less as compared with fastback end. These results are demonstrated by pressure distribution and velocity distribution which offer a good understanding of the flow behavior around the vehicle bodies.

Keywords: computational fluid dynamic, k-ε turbulence model, numerical simulation, wake region.

تأثير اشكال المركبات على منطقة الضغط المنخفض و معامل الكبح: دراسة عددية

حيدر كريم سكران

مدرس مساعد

كلية الهندسة/ جامعة المثنى

الخلاصة

ان الغرض من هذه الدراسة هو الحصول على مفهوم افضل حول منطقة الضغط المنخفض او ما تسمى بمنطقة الضعف المتولدة في الاجزاء الخلفية للمركبات بسبب تأثير ديناميكية الهواء عند جريانه حول المركبات اثناء حركتها. ان الهدف الرئيسي لهذه الدراسة هو مناقشة تأثير الشكل الخارجي للمركبات على منطقة الضغط المنخفض و كذلك على معامل الكبح . تُستخلص النتائج باختبار شكلين مختلفين من المركبات و حسب تصميمهما الخارجي وهما الاشكال ذات النهايات السريعة (Fastback) و الاشكال ذات النهايات المثلومة (Notchback). سَتُوظف هذه الدراسة بواسطة ديناميكية الموائع الحسابية (CFD) باستعمال برنامج المحاكاة (STAR-CCM+[®] software). تعتمد هذه الدراسة الجريان الاضطرابي المستقر (steady turbulent flow) باستعمال معادلات الجريان الاضطرابي (k-epsilon turbulence models). وقد اظهرت النتائج المستحصلة من المحاكاة ان اختلاف منطقة فصل الهواء خلف المركبة يعزى الى اختلاف تصميم هيكل المركبة. و يمكن الحصول على اقل معامل للكبح في الاشكال ذات النهايات المثلومة (Notchback) لان منطقة فصل الهواء تكون اقل في هذه الاشكال مقارنة مع الاشكال ذات النهايات السريعة (Fastback). و برهنت منحنيات توزيع الضغط و السرعة التي تم الحصول عليها من خلال المحاكاة صحة النتائج وبدورها تساعد على فهم سلوك جريان الهواء حول هياكل المركبات.

الكلمات الرئيسية: ديناميكية الموائع الحسابية, معادلات الجريان الاضطرابي, دراسة عددية و منطقة الضعف.

1. INTRODUCTION

Automobiles companies produce too many differences of body designs, and every design has specific features. However, people do not know the benefits of these designs because they look for the beautiful shape with appropriate cost when they decide to buy a car.

When vehicles move, air flows over the outer circumference of the vehicle. The air is distributed with different magnitude of velocities behind the body of the vehicle as shown in **Fig.1**.

The separation will happen when the fluid flow does not follow the shape of the surface so it detaches or separates, causing the wake region to be generated in the rear end of the vehicle, **Hucho, 2013**, and **Katz, 2006**. This region will be developed behind the vehicle body because of the separation of the air at the back of the vehicle. A separation causes two regions depending on their location from the rear of the car. The first region, which is developed when the separation happened close behind the vehicle, is known as the near wake region, and the second one, which is developed when the separation happened further behind the vehicle, is known as the far wake region as shown in **Fig.2**.

The structure of the vortex depends on the geometry of the vehicle and the history of its upstream flow, the geometry also affects the relative size of the wake region as shown in **Fig.3**. A lot of investigations have been employed to study the effect of the geometry of the moving bodies on the aerodynamic performance especially for the automobiles since it has a very significant relation with the fuel consumption. The aerodynamic drags of a road vehicle are responsible for a huge part of the vehicle fuel consumption and cause up to 50% of the total vehicle fuel consumption at highway speeds, **Sudin, et al. 2014**. The rear end shape has a worthy relation with the drag and it can help to design an acceptable shape with minimum rear lifts without increasing the drag coefficient, **Fukuda, et al. 1995**. The investigation of the stability characteristic of Notchback- type vehicle under the influence of transient aerodynamics by Large-Eddy Simulation (LES) turbulence model shows a strong impact on unsteady flow structure around the rear end of the vehicle **Cheng, et al., 2011**. The mean pressure results show a significant increment in the base pressure with the drag reduction which strongly influences the unsteady base pressure and velocity spectral at a Strouhal number- which is a useful dimensionless value for analyzing oscillating unsteady fluid flow in dynamics problems - of 0.07, **Khalighi, et al., 2001**.

The time average analysis expresses a strong interaction among boundary layers, drag coefficient and pressure at the rear end of the vehicle, **Vanraemdonck, and Vantooten, 2008**. It is obvious that the topological features of the time-average flow are independent of the averaging time T and grid-size, **Franck, et al., 2009**. The time-averaged structure of the wake of a fastback type road vehicle has a pair of vortices placed one above another. The trailing edges of these vortices are parallel to the longitudinal axis of the vehicle, **Ahmed, 1983**.

A lot of turbulence models have been investigated to analyze the air attitude at the rear end of the vehicles. The numerical simulation using shear stress transport turbulence model can predict recirculation which is more intensive and it can give results which are very close to the experimental investigations in their accuracy, **Guilmineau, 2003**. The examination of the aerodynamic damping mechanism- which is the reduction of vibrations by the inherent stability of a body or of its control surface- in sedan-type vehicle shows that the unsteady aerodynamics is apparent as having undesirable effect on vehicles stability. Investigating LES turbulence model shows an important influence of transient flow structure above the rear section of the sedan- type vehicle, **Cheng, et al., 2011**. Wall boundary cases with separation and reattachment using the Durbin's $k-\epsilon-v^2$ turbulence model give very good accurate results. The turbulence model and the



near wall grid are not the only parameters that can affect the results of the drag coefficient. It is possible to make the CFD more accurate with a suitable selection of a different scheme, **Liu, and Alfred, 2003**.

This work tackles the effect of different vehicle geometry on the airflow attitude in the wake region and calculates the aerodynamic drag coefficient. It takes the three most common body geometries of the small car which are fastback, square back, and notchback as shown in **Fig.4**. All these designs have the same shape of the front region, which is so close to Ahmed body, but with different design of the back section. Every design has a specific effect on the aerodynamic features when the air flows over these bodies.

It focuses on the near wake region of two different geometries, which are the fastback and the notchback because the square back and the fastback have a common parameter (slant angle) which is considered to be 25 degrees close to the fastback shape as shown in **Fig.5**. The simulation has been achieved by using a computational fluid dynamics code, STAR-CCM+, to simulate the flow around bodies. Pressure distribution, velocity vector, and the drag coefficient that developed behind the body of the vehicle are collected after the simulation done to have a good understanding about the effect of the vehicle geometry on the drag coefficient and other results.

2. PROBLEM DEFINITION

The three-dimensional domain has been generated with structural hexahedral mesh. The boundary layers have been resolved using trimmer mesh, 0.4 m base size, and 7 prism layers to study the boundary conditions carefully. The computational domain is generated with 8m long, 0.4m wide and 3m high. Furthermore, the fastback geometry is 1.044m long, 0.288 m high and 0.4 m wide. The notchback geometry size is 1.184m long, 0.288 m high and 0.4 m wide as shown in **Figs.6, 7, and 8**. Because the three-dimensional domain is very complicated, the simulation will take more time to be achieved. Thus, the computational domain is converted to two-dimensional one which is more suitable in this study since the body is symmetry with the z-direction as shown in **Fig.9**. The structural mesh consists of 13389 cells, 377490 faces, and 19022 vertices as shown in **Figs.10, and 11**. The boundary conditions and the turbulence model ($k-\epsilon$) have been used to solve the problem. The problem is carried out as a bluff body that is much close to Ahmed body. A fully submerged with the surrounding air has been assumed. The numerical analysis is employed to emphasize the near wake region and to study its effect on the airflow behavior and the drag coefficient magnitude.

The two-dimensional geometry has been created by using STAR-CCM+® to simulate a steady state conditions and incompressible fluid flow problem. The problem specification and the boundary conditions are explained in **tables 1, and 2** for the two cases.

3. TURBULENCE MODELS

STAR-CCM+® software is one of the CFD commercial tools that are used to simulate problems and to solve the governing equation for the flow around the vehicle body and other computational fluid dynamics problems relying on the boundary conditions. The Navier-Stoke equation is a complex equation that has a lot of unknown terms and its calculation needs to apply turbulence model to be solved. Air flow over the vehicle is governed by Reynolds Average Navier-Stokes equations (RANS) in order to study the flow around the vehicle as explained below:



$$\frac{\partial p}{\partial t} + \text{div}(\rho U) = 0 \quad (1)$$

$$\rho \frac{\partial U_i}{\partial t_i} + \rho \frac{\partial}{\partial x_j} (U_i U_j + \overline{u'_j u'_i}) = -\frac{\partial P}{\partial x_i} + \frac{\partial}{\partial x_j} (2\mu S_{ij}) \quad (2)$$

The term $(\overline{u'_j u'_i})$ is known as the Reynolds stress tensor which is also considered as stress term due to fluctuating velocities.

Boussinesq assumption has been applied to compute Reynolds stress tensor.

$$-\rho \overline{u'_j u'_i} = \mu_t \left[\frac{\partial U_i}{\partial x_i} + \frac{\partial U_j}{\partial x_j} \right] - \frac{2}{3} \rho k \delta_{ij} = 2\mu_t \delta_{ij} - \frac{2}{3} \rho k \delta_{ij} \quad (3)$$

The software has been set up with k-ε turbulence model to solve the governing equation directly. The k-ε turbulence model has two model equations which are the turbulence kinetic energy k and its dissipation rate ε. It is widely used to have a better result and to enhance the stability with convergence.

The k and ε have been employed to describe velocity scale \mathcal{G} and length scale ℓ as follows:

$$\mathcal{G} = k^{1/2} \quad (4)$$

$$\ell = \frac{k^{2/3}}{\varepsilon} \quad (5)$$

The eddy viscosity can be specified by applying the dimensional analysis as follows:

$$\mu_t = C_\mu \rho \mathcal{G} \ell = \rho C_\mu \frac{k^2}{\varepsilon} \quad (6)$$

C_μ is a dimensionless constant, it equals to 0.09.

The transport equations for k and ε can also be specified as follows:

$$\frac{\partial(\rho k)}{\partial t} + \text{div}(\rho k U) = \text{div} \left[\frac{\mu_t}{\sigma_k} \text{grad} \cdot k \right] + 2\mu_t S_{ij} \cdot S_{ij} - \rho \varepsilon \quad (7)$$

$$\frac{\partial(\rho \varepsilon)}{\partial t} + \text{div}(\rho \varepsilon U) = \text{div} \left[\frac{\mu_t}{\sigma_\varepsilon} \text{grad} \cdot \varepsilon \right] + C_{1\varepsilon} \frac{\varepsilon}{k} 2\mu_t S_{ij} \cdot S_{ij} - C_{2\varepsilon} \rho \varepsilon \frac{\varepsilon^2}{k} \quad (8)$$

$\sigma_k = 1.00$, $\sigma_\varepsilon = 1.30$, $C_{1\varepsilon} = 1.44$, $C_{2\varepsilon} = 1.92$ all of these terms are adjustable constants.

4. RESULTS AND DISCUSSION

After completing mesh generation, the solution has been obtained when the convergence is done. The solution has two different groups of results depending on the conditions of the problem. The drag coefficient C_D is computed as follows:

$$C_D = \frac{F_D}{\frac{1}{2} \rho U^2 A_x} \quad (9)$$

F_D is the drag force, ρ is the fluid (air) density, U is the upstream velocity, and A_x is the projected area of the body in x direction. C_k , C_B , C_s , and C_D represent the drag coefficient at the nose, back, the rear slope and the total, respectively.

The simulation reached to convergence in approximately 57000 times of iterations for the notchback and 58000 times of iterations for the fastback, this happened because each problem has its boundary conditions specially the shape of the geometry. The simulation has done with convergence the results as shown in **Figs.12** and **13** that show the residual for the problem simulation.

Figs.14 and **15** shows the drag coefficient for different places of the vehicle body since the body has been divided into three places which are nose, slope, and back as shown in **Fig.16** and each one has individual magnitude of the drag.

This study focuses on the drag value and compares the computed results for two models. The drag value can be computed from Eq. (9); however, in this study the results of the drag coefficients are obtained from **Figs.14** and **15** since they are clear to be mentioned. **Tables 3** and **4** show the results of the drag coefficient for the specific problem. The total drag coefficient for the fastback is 0.698 and for the notchback is 0.654.

Figs.17 and **18** explain the pressure contour for the vehicle body that moves through the air and they display the behavior of the pressure distribution for the entire body. The differentiation of the pressure distribution is considered at the wake region since the difference between the two cases is restricted at the rear region.

Figs.19 and **20** show the velocity contour of the airflow over the entire body and it is easy to mention that the velocity at the wake region for the notchback is less than the velocity for the fastback.

In addition, **Figs .21, 22, 23,** and **24** that show velocity magnitude and velocity vector can confirm the results. The pressure at wake region for the notchback is more than the pressure at the wake region for the fastback. *“Pressure is low at locations where the flow velocity is high, and pressure is high at locations where the flow velocity is low”*. **Cengel, and Cimbala, 2006**.

Fig.25 shows a comparison of the two trailing vortexes in the near wake for both models which is clearly defined in these plots. It can be observed that the recirculation region for the fastback is bigger than the recirculation region for the notchback and it is obvious to understand that the drag coefficient for the fastback is bigger.



The shape of the rear edge of the bodies controls the velocity and pressure distribution in this region then affects the drag value for the total body.

5. CONCLUSIONS

In the present paper, the performance of airflow over different geometries of vehicle bodies which are the notchback and the fastback at the same boundary conditions, has been investigated numerically by Computational Fluid Dynamics (CFD) using k- ϵ turbulent models and the simulation was made by STAR-CCM+[®] software. The simulation shows strong results of the effect of the geometries on the drag coefficient and the air attitude in the back region of vehicles.

Figures and analysis in this study reveal the effects of the back end configuration on the flow field, drag coefficient, and air separation for body of vehicles, it is probable to conclude that:

1. The notchback end has a less drag coefficient and less area of separation than that for fast back end. This is because of the difference in shape especially in the rear back.
2. The results achieved were very in agreement with the theoretical understanding of the air flow over bodies.
3. Air and any other fluid attitudes depend on the shape of the body that the fluid would flow over it.

REFERENCES

- Ahmed, S. R., 1983, *Influence of Base Slant on the Wake Structure and Drag of Road Vehicle*, Transaction of ASME, Journal of Fluid Engineering, vol.105, PP. 429-434.
- Cengel, Y., and Cimbala, J., 2006, *Fluid mechanics: Fundamentals and applications*, McGraw-Hill, New York.
- Cheng, S. Y., Tsubokura, M., Nakashima, T., Nouzawa, T. and Okada, Y., 2011, *A Numerical Analysis of Transient Flow Past Road Vehicles Subjected to Pitching Oscillation*, Journal of Wind Engineering and Industrial Aerodynamics, vol. 99, No.5, PP. 511-522.
- Cheng, S. Y., Tsubokura, M., Nakashima, T., Okada, Y., and Nouzawa, T., 2011, *Large Eddy Simulation of Flow Past Road Vehicles Subjected to Pitching Oscillation*, 20th AIAA Computational Fluid Dynamics Conference.
- Fukuda, H., Yanagimoto, K., China, H., and Nakagawa, K., 1995, *Improvement of Vehicle Aerodynamics by Wake Control*, JSAE review, vol. 6, No.2, PP.151-155.
- Franck, G., Nigro, N., Storti, M., and D'elia, J., 2009, *Numerical Simulation of the Flow Around the Ahmed Vehicle Model*, Latin American applied research, vol.3, No.4, PP. 295-306.
- Guilmineau, E., 2003, *Numerical Simulation of Flow around a Simplified Car Body*, ASME/JSME 4th Joint Fluids Summer Engineering Conference, American Society of Mechanical Engineers.



- Hucho, W., 2013, *Aerodynamics of Road vehicles: from Fluid Mechanics to Vehicle Engineering*, Elsevier.
- Katz, J., 2006, *Race Car Aerodynamics: Designing for Speed*, Bentley Publisher.
- Khalighi, B., Zhang, S., Koromilas, C. , Balkanyi, S. R. , Luis P. B., Iaccarino, G. and Moin, P., 2001, *Experimental and Computational Study of Unsteady Wake Flow behind a Bluff Body with a Drag Reduction Device*, SAE Technical Paper.
- Liu, Y., and Alfred. M., 2003, *Numerical Modeling of Airflow over the Ahmed Body*, Proceedings of the 11th Annual Conference of the CFD Society of Canada.
- Richards, K. A., 2000, *Computational Modeling of Pollution Dispersion in the Near Wake of a Vehicle*, Proceedings of the MIRA international conference on aerodynamics.
- Sudin, M. N., Abdullah, M. A., Shamsuddin, S.A., Ramli, F. R. and Tahir, M. M., 2014, *Review of Research on Vehicles Aerodynamic Drag Reduction Methods*, International Journal of Mechanical & Mechatronics Engineering, Vol. 14, No. 2, PP. 35-47.
- Vanraemdonck, G. M. R., and Vantooten, M. J. L., 2008, *Time-averaged Phenomenological Investigation of a Wake behind a Bluff Body*, BBAA VI International Colloquium on: Bluff Bodies Aerodynamics & Applications. Vol. 51.

NOMENCLATURE

A_x = projected area of the body in x direction, m^2 .

C_D = the total drag coefficient.

C_k = the nose drag coefficient.

C_B = the back drag coefficient.

C_s = the slope drag coefficient.

C_{μ} , σ_{ϵ} , $C_{1\epsilon}$, $C_{2\epsilon}$, σ_k = model constants.

F_D = the drag force, N.

L = characteristic length, m.

S_{ij} = the strain rate tensor, 1/s.

U = the upstream velocity, m/s.

u = velocity, m/s.

Greek symbols.

ϵ = turbulent dissipation rate, m^2/s^3 .

k = turbulent kinetic energy, m^2/s^2 .

ℓ = turbulent length scale, m.

μ_t = turbulent viscosity, Ns/m^2 .

ρ = density of the air, kg/m^3 .

ν = kinematic viscosity, m^2/s .

ϑ = velocity scale, m/s .

**Subscripts**

$i; j$ = referring x- and y-directions respectively.

Table1. Fluid properties.

Fluid properties	
Fluid/Material	Air
Density	Constant, $\rho = 1.225 \text{ kg/m}^3$
Velocity	40 m/s
Time domain	steady
Turbulence model	k- ϵ turbulence model

Table 2. The simulation settings.

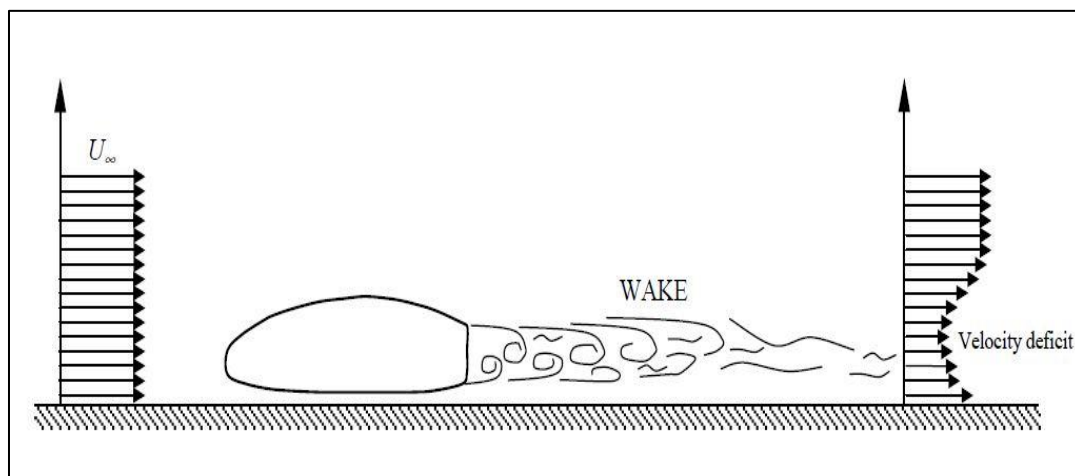
Simulation Settings	
Domain	Two Dimensional
Density	Constant, $\rho = 1.225 \text{ kg/m}^3$
Velocity	40 m/s
Time domain	Steady
Turbulence model	k- ϵ turbulence model
Solver	Segregated
Fluid/Material	Air
Mesh properties	Trimmer mesh, 7 prism layers; Base size 0.4m

Table 3. The results of the drag coefficient for fastback.

Drag Coefficient for Fastback	
C_D	0.698
C_B	0.248
C_K	0.125
C_S	0.325

Table 4. The results of the drag coefficient for notchback.

Drag Coefficient for Notchback	
C_D	0.654
C_B	0.236
C_K	0.175
C_S	0.243

**Figure 1.** A wake region behind the vehicle, **Katz, 2006.**

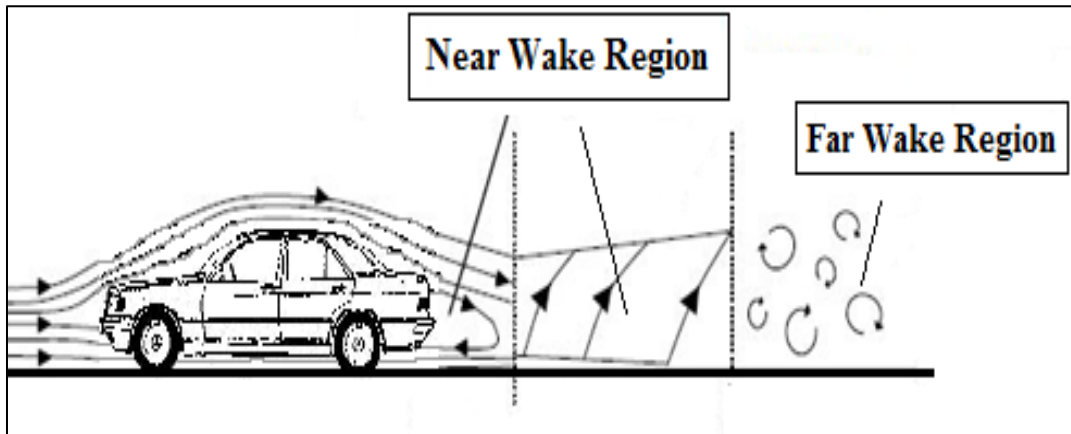


Figure 2. The near and the far wake regions, Richards, 2000.

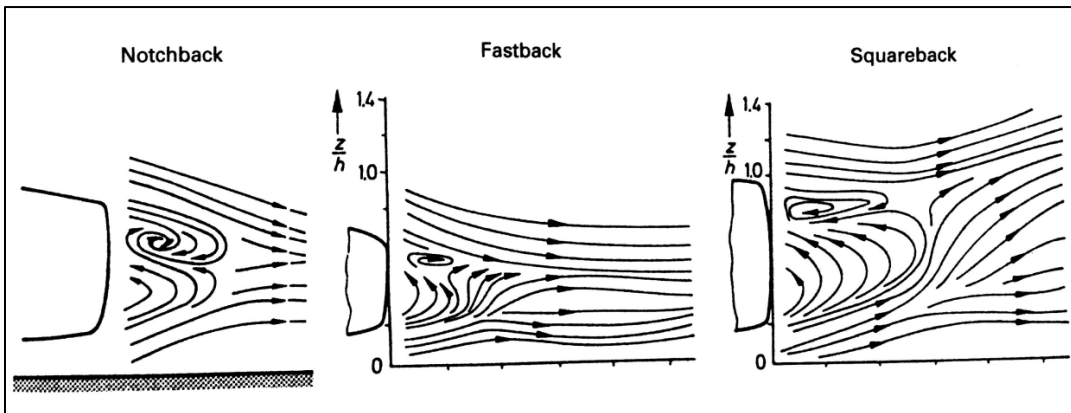


Figure 3. Vortices behind the vehicles, Hucho, 2013.

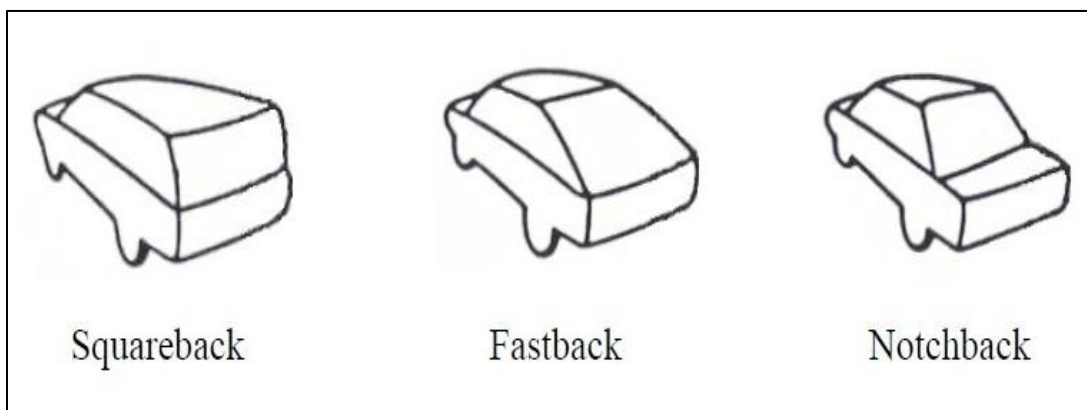


Figure 4. The common body geometries for the small car, Richards, 2000.

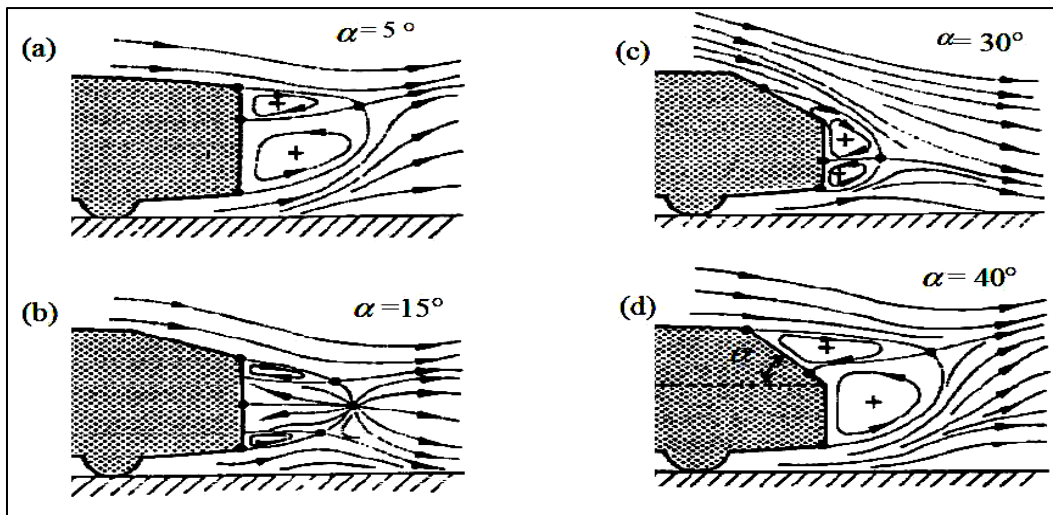


Figure 5. Different base degree of Slant angle, Ahmed, 1983.

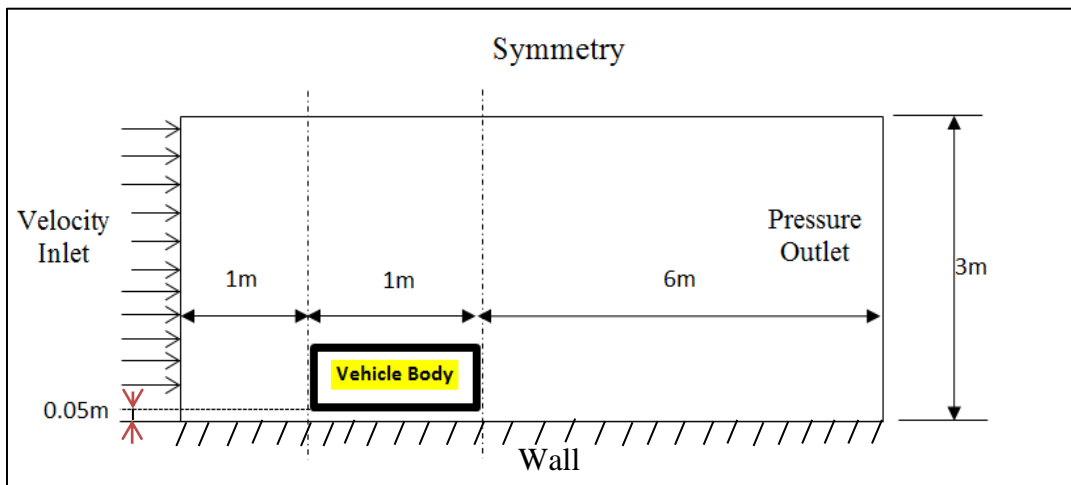


Figure 6. 2D Computational domain.

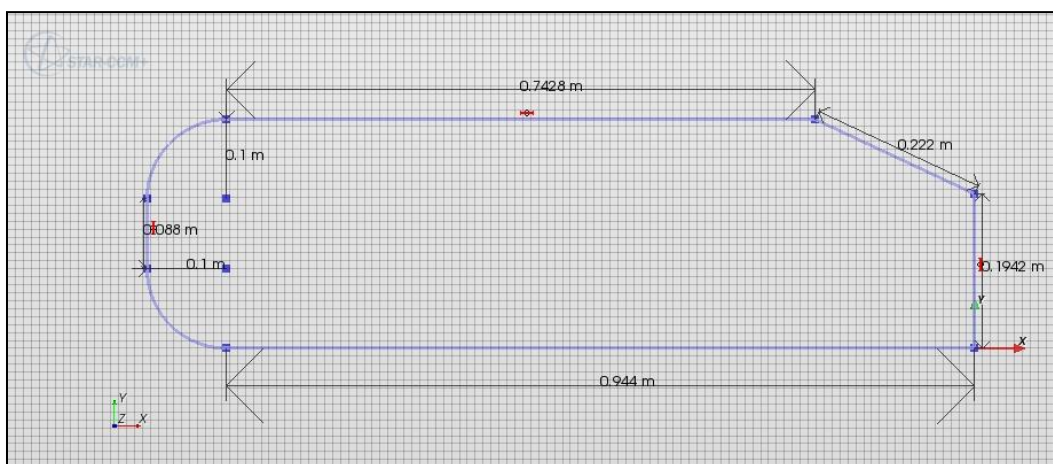


Figure 7. The cross-section of fastback geometry with 25 slant angle degree.

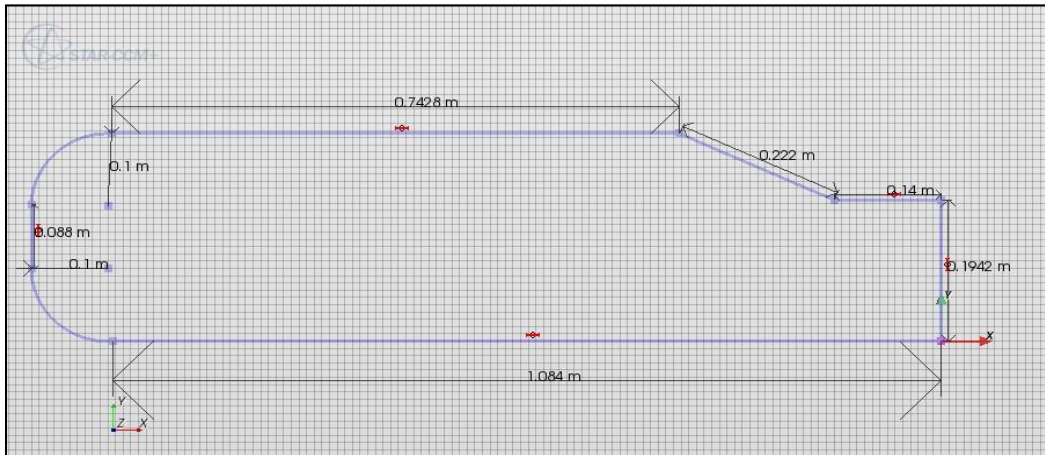


Figure 8. The cross-section of notchback geometry with 25 slant angle degree.

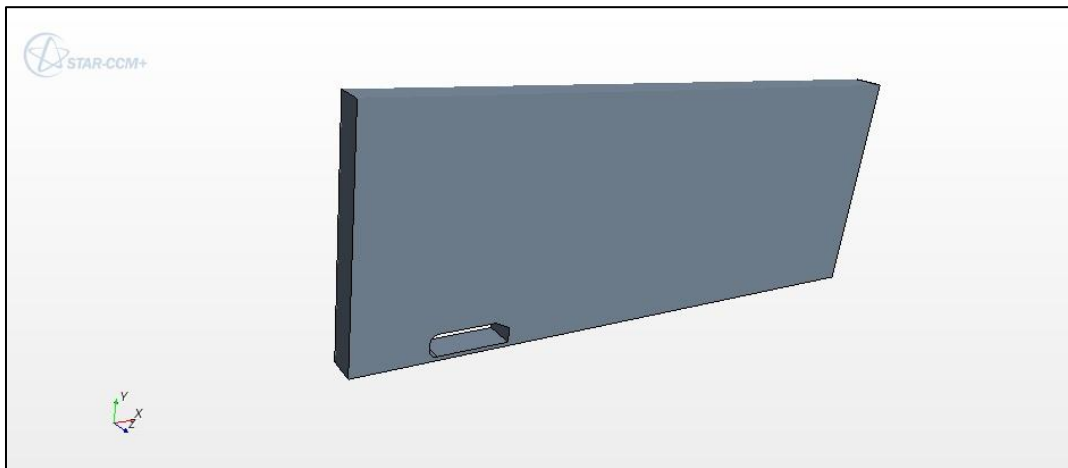


Figure9. The 3D computational domain.

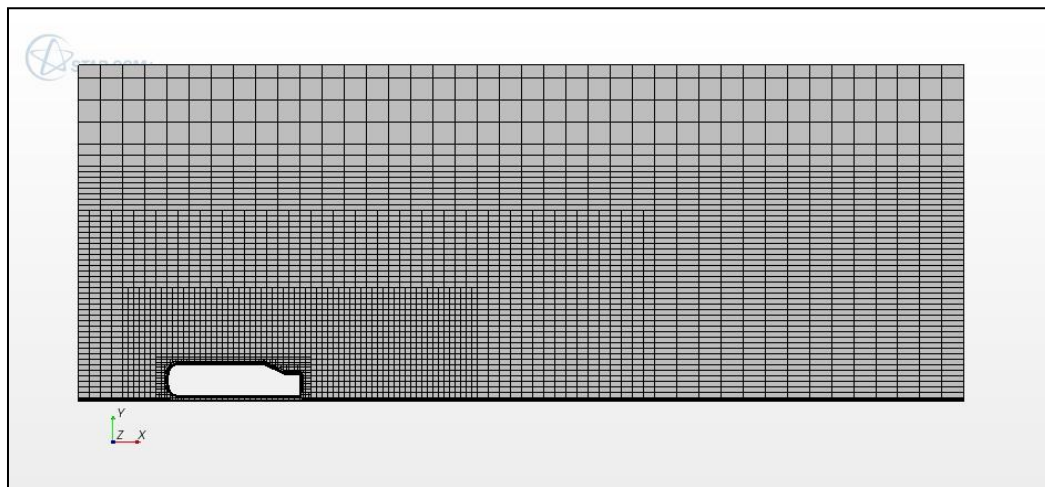


Figure 10. The cross-section of notchback geometry with 0.4 mesh base size.

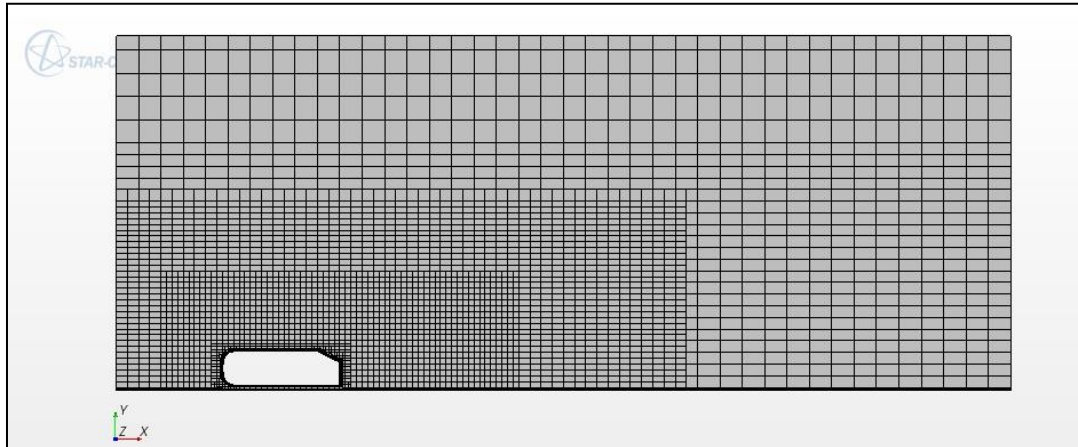


Figure 11. The cross-section of fastback geometry with 0.4 mesh base size.

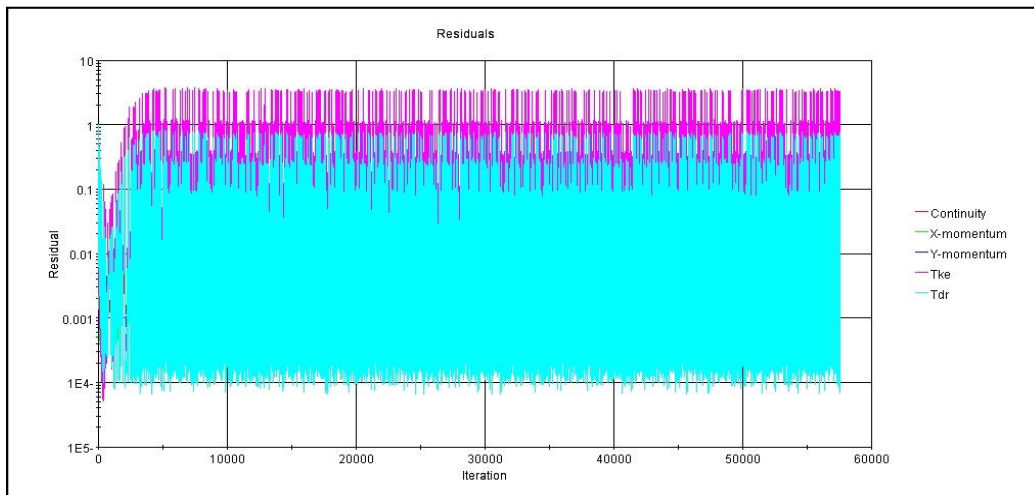


Figure 12. Residual history for fastback.

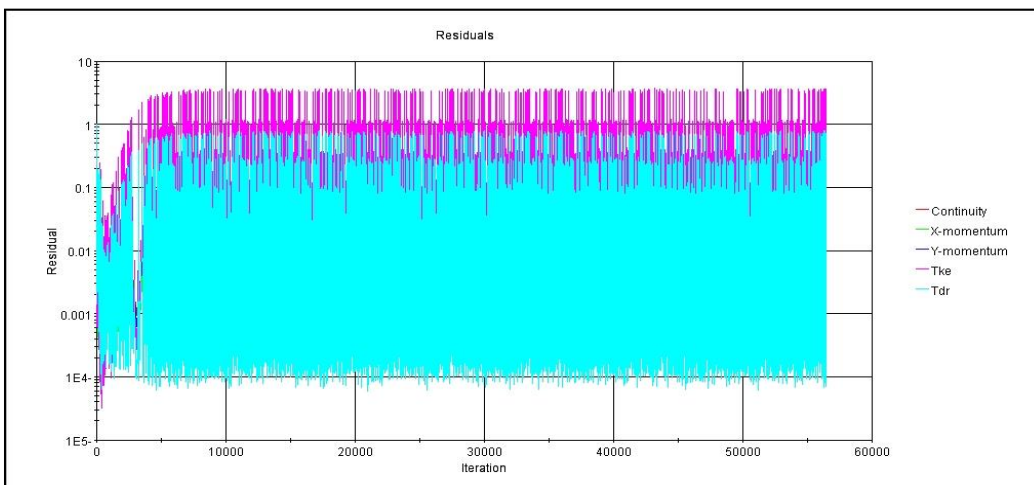


Figure 13. Residual history for notchback.

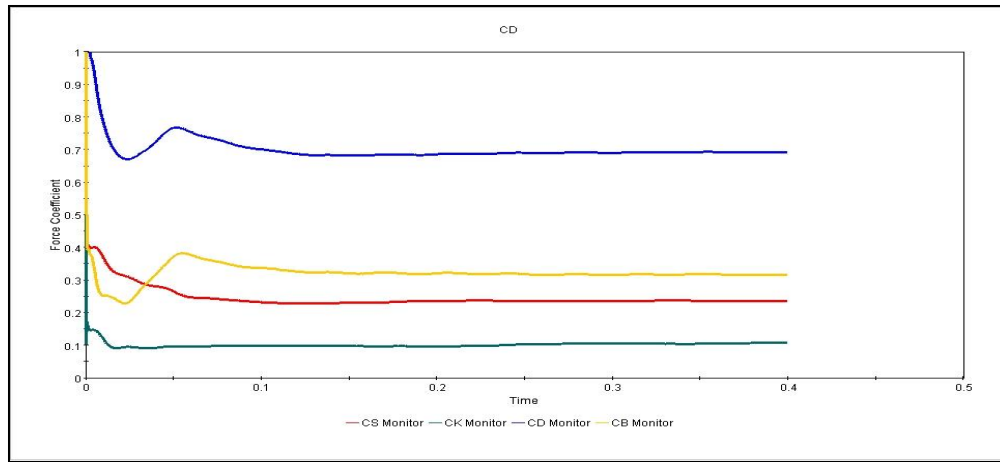


Figure 14. Drag coefficient for fastback.

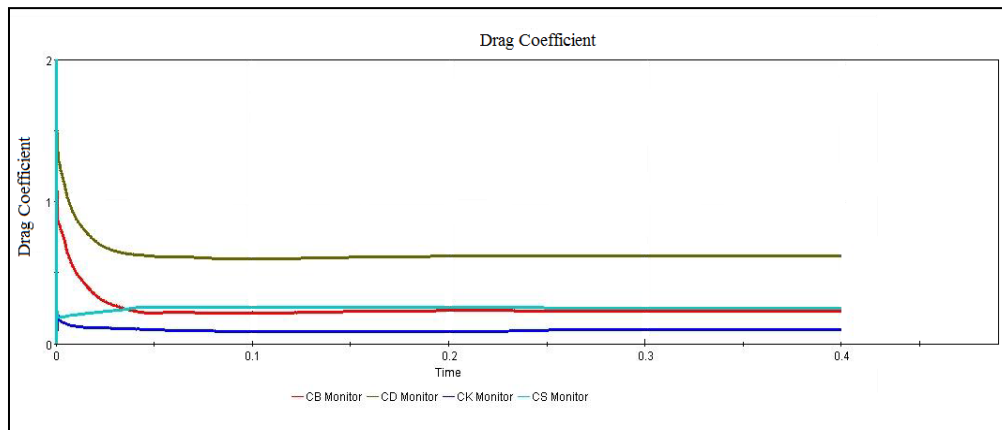


Figure 15. Drag coefficient for notchback.

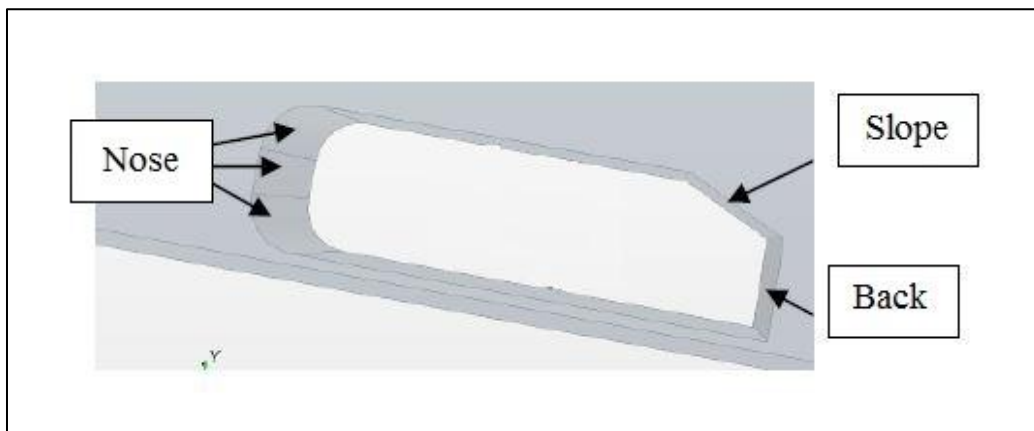


Figure 16. Divisions of the experimental area of the body.

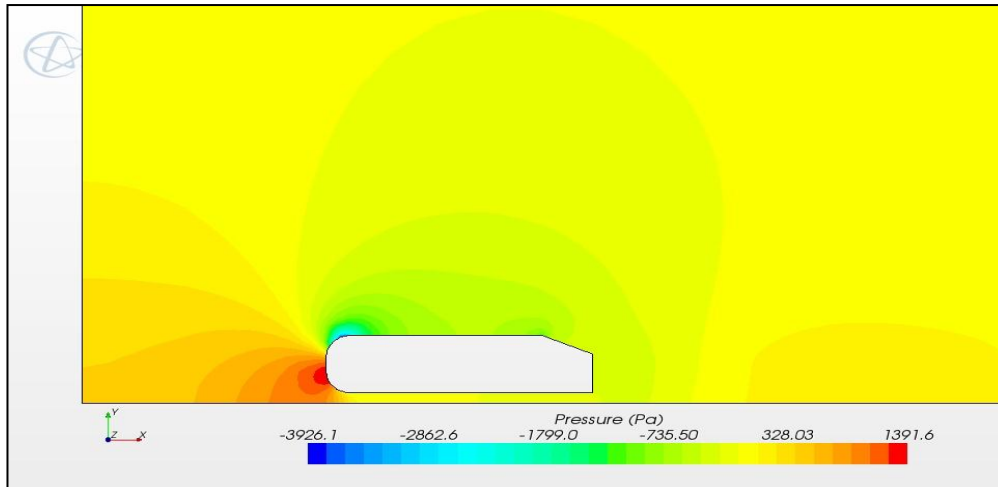


Figure 17. Pressure Contour for fastback.

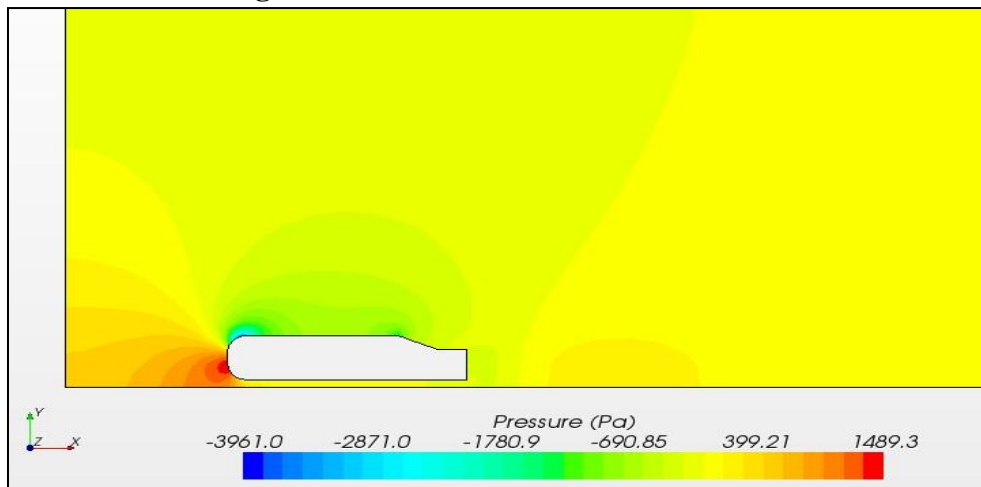


Figure 18. Pressure contour for notchback.

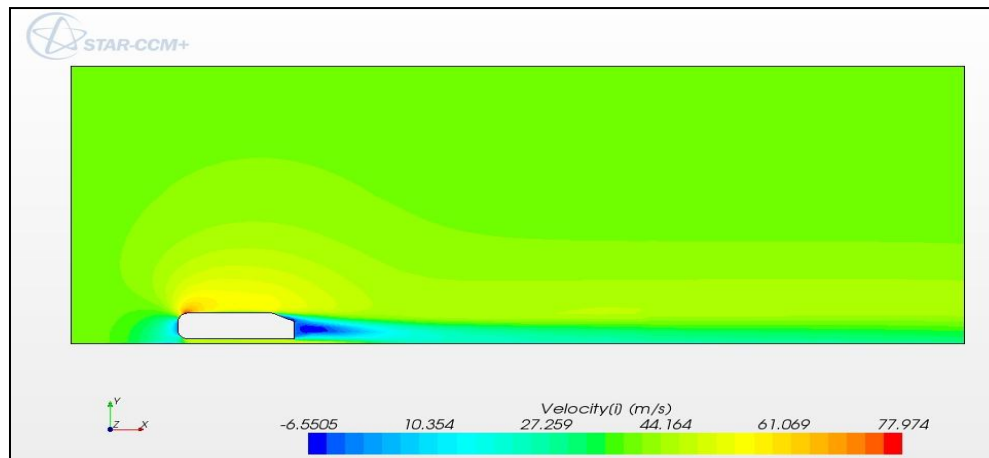


Figure 19. Velocity contour for fastback.

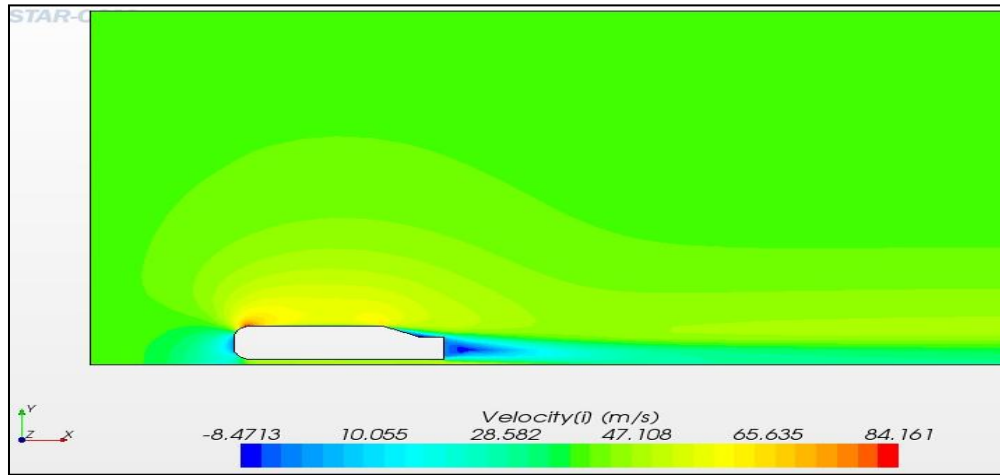


Figure 20. Velocity contour for notchback.

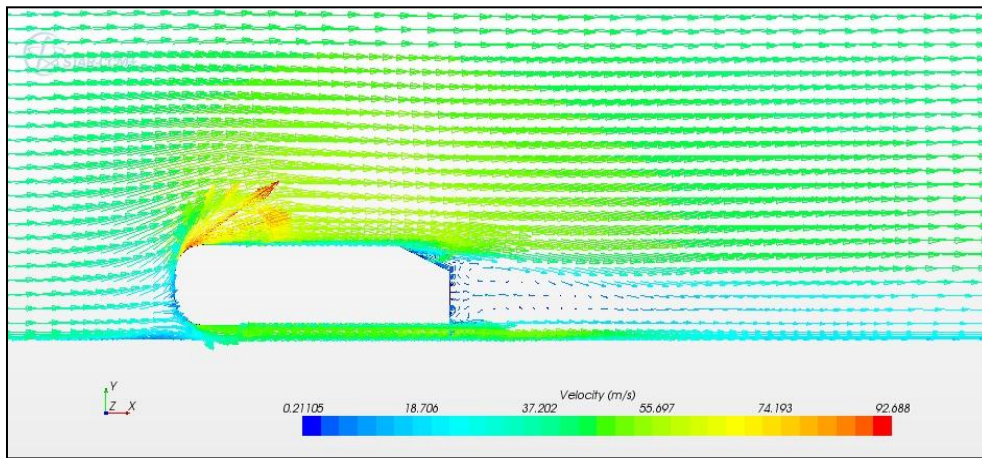


Figure 21. Velocity vectors for fastback.

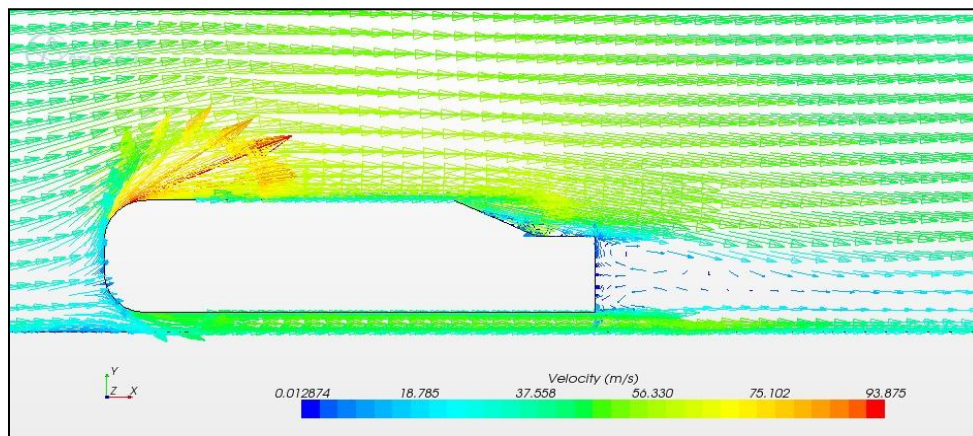


Figure 22. Velocity vector for notchback.

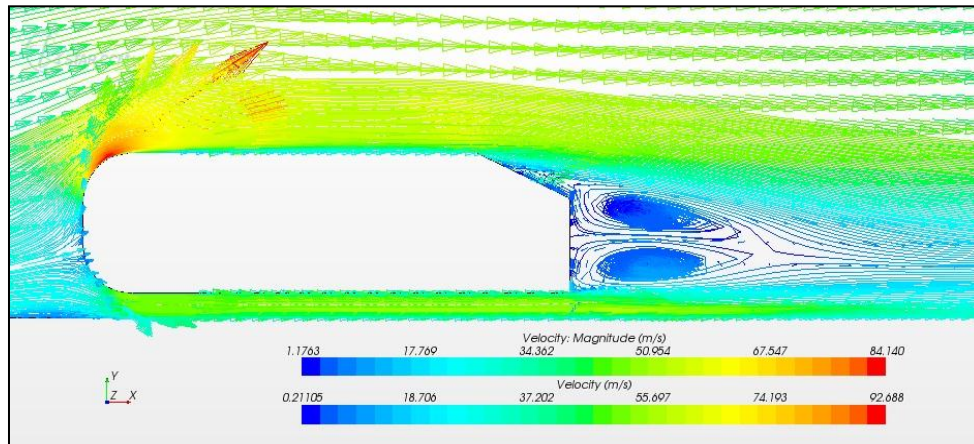


Figure 23. Velocity magnitude for fastback.

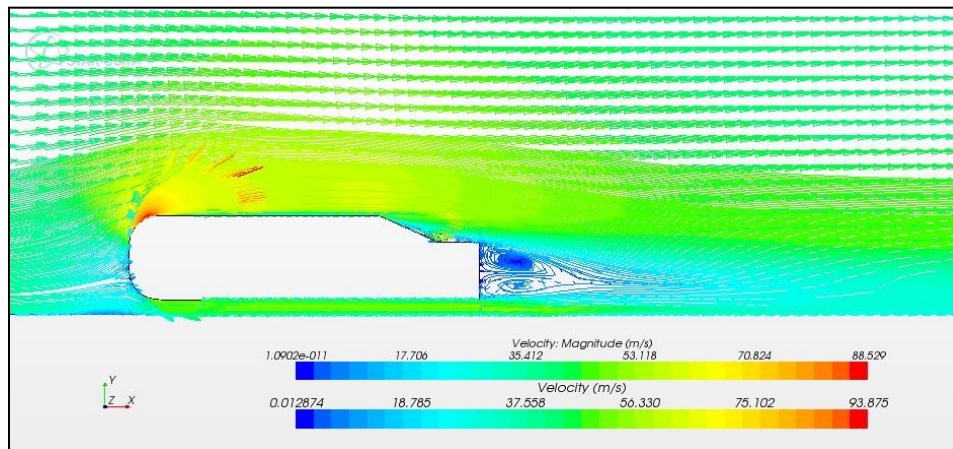


Figure 24. Velocity magnitude for notchback.

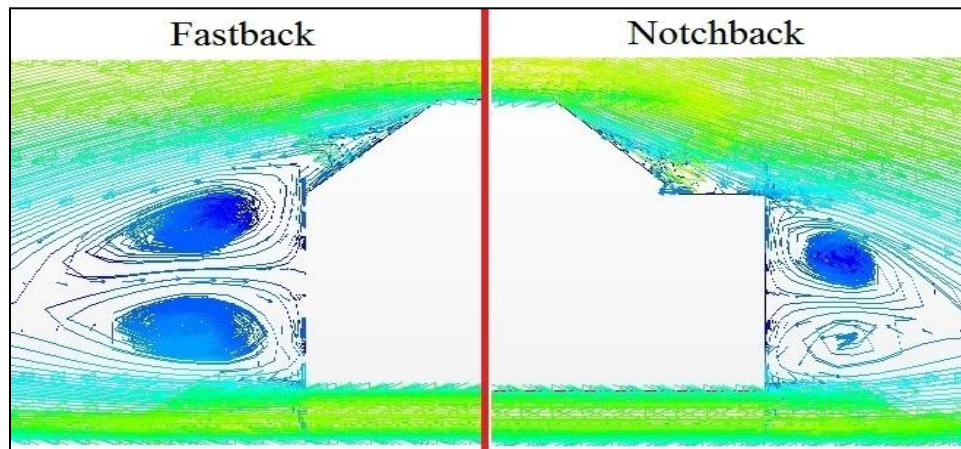


Figure 25. Comparing the wake region between the fastback and the notchback.